Virology 452-453 (2014) 12–22

Contents lists available at ScienceDirect

Virology

journal homepage: www.elsevier.com/locate/yviro

Foot-and-mouth disease virus virulence in cattle is co-determined by viral replication dynamics and route of infection

Jonathan Arzt, Juan M. Pacheco, George R. Smoliga, Meghan T. Tucker, Elizabeth Bishop, Steven J. Pauszek, Ethan J. Hartwig, Teresa de los Santos, Luis L. Rodriguez*

From the Plum Island Animal Disease Center, Foreign Animal Disease Research Unit, Agricultural Research Service, United States Department of Agriculture, Plum Island, NY, USA

ARTICLE INFO

Article history:
Received 14 October 2013
Returned to author for revisions
27 December 2013
Accepted 2 January 2014
Available online 25 January 2014

Keywords:
Attenuation
Bovine
Cattle
FMD
FMDV
Foot-and-mouth
Interferon
Pathogenesis
Virulence
Virus

ABSTRACT

Early events in the pathogenesis of foot-and-mouth disease virus (FMDV) infection in cattle were investigated through aerosol and intraepithelial lingual (IEL) inoculations of a cDNA-derived FMDV-A_{24} wild type virus (FMDV-WT) or a mutant derived from the same clone (FMDV-Mut). After aerosolization of FMDV-WT, primary infection sites had significantly greater quantities of FMDV, viral RNA, and type I/III interferon (IFN) activity compared to corresponding tissues from cattle infected with FMDV-Mut. Additionally, FMDV-WT-infected cattle had marked induction of systemic IFN activity in serum. In contrast, FMDV-Mut aerosol-infected cattle did not manifest systemic IFN response nor had viremia. Interestingly, IEL inoculation of FMDV-Mut in cattle restored the virulent phenotype and systemic IFN response. These data indicate that the attenuated phenotype in cattle is associated with decreased replicative efficiency, reflected by decreased innate response. However, attenuation is abrogated by bypassing the common primary infection sites, inducing accelerated viral replication at the inoculation site.

Published by Elsevier Inc.

Introduction

Foot-and-mouth disease virus (FMDV; family *Picornaviridae*; genus *Aphthovirus*) is the cause of a highly contagious, acute disease of cloven-hoofed animals characterized by fever, lameness, and vesicular lesions of the feet, tongue, snout, and teats (Alexandersen et al., 2003; Arzt et al., 2011b; Grubman and Baxt, 2004). In recent years there have been several breakthroughs in elucidating functions of FMDV proteins (Borca et al., 2012; Gladue et al., 2012; Lawrence et al., 2012; Pacheco et al., 2013); yet, the FMDV leader protein, L_{pro}, remains the most thoroughly investigated determinant of virulence (reviewed in (Arzt et al., 2011a)). Virus constructs lacking the L_{pro} sequence (leaderless FMDV) have been shown to be avirulent in cattle and pigs (Brown et al., 1996; Chinsangaram et al., 1998; Uddowla et al., 2012). Cattle exposed to leaderless FMDV by aerosol do not develop viremia or clinical signs of FMD (Brown et al., 1996; Uddowla et al., 2012) and have minimal quantities of viral RNA (vRNA) detected in lungs by *in situ* hybridization (ISH) and no vRNA detected in any other tissues (Brown et al., 1996). More recently, FMDV mutants with in-frame insertions in L_{pro} were shown to be markedly attenuated in cattle (Piccone et al., 2010b). These viruses had a more extensive dissemination within the respiratory tract (compared to leaderless FMDV) after aerosol inoculation in cattle; but, similar to the leaderless virus, neither viremia nor clinical disease were detected (Brown et al., 1996; Piccone et al., 2010b). The complete attenuation of this mutant virus which contained and expressed all viral genes provided a unique opportunity to investigate the early events in FMDV pathogenesis as described herein.

The modulation of transcription of interferons (IFN) and IFN-stimulated genes (ISG) in the early innate response of cattle to FMDV infection has been recently described (Diaz-San Segundo et al., 2011; Perez-Martin et al., 2012; Stenfeldt et al., 2012; Zhang et al., 2006). These works have demonstrated that type I/III IFN activity, measured using an Mx-CAT reporter system, is detectable in serum of unvaccinated, FMDV-infected cattle with onset and duration similar to that of viremia (Howey et al., 2012; Perez-Martin et al., 2012; Stenfeldt et al., 2011). Additionally activation of ISG pathways in cattle subsequent to exogenous delivery of recombinant vectors expressing type I (e.g. IFN-α) and type III (IFN-λ) IFN has been characterized (Diaz-San Segundo et al., 2011;

* Correspondence to: USDA, ARS-NAA, PIADC, 40550 Rt. 25, Orient Point, New York 11957, USA. Tel.: +1 631 323 3364; fax: +1 631 323 3006.
E-mail address: luis.rodriguez@ars.usda.gov (L.L. Rodriguez).

0042-6822/$ - see front matter Published by Elsevier Inc.
http://dx.doi.org/10.1016/j.virol.2014.01.001

Perez-Martin et al., 2012). These works have demonstrated that FMDV infection (Perez-Martin et al., 2012) and/or delivery of recombinant vectors expressing IFN transgenes (Diaz-San Segundo et al., 2011) result in induction of transcription of various ISGs in peripheral blood mononuclear cells (PBMC) and tissues of cattle that have been demonstrated to be sites of primary infection by FMDV (Arzt et al., 2010; Pacheco et al., 2010a). ISGs that were substantially induced included IRF-7, CCL-2, ISG-15, Mx-1, OAS1, PKR, and RIG1 (Diaz-San Segundo et al., 2011; Perez-Martin et al., 2012).

Recent reports from our laboratory have described a novel method for aerosol inoculation of cattle with FMDV together with trimodal FMDV detection systems, and the utility of using these systems for investigation of FMD pathogenesis *in vivo* (Arzt et al., 2010; Pacheco et al., 2010a). These works demonstrate that subsequent to aerosolization of cattle with FMDV-O_1-Manisa, the previremic events consist of primary infection in epithelial crypts of the nasopharynx followed by extensive amplification in the pneumocytes in the lungs and the establishment of viremia. In the current study, we utilized similar experimental systems to characterize early events in the pathogenesis of FMDV-A_{24}-Cruzeiro (FMDV-WT) (Rieder et al., 2005) and contrast with that of an Lpro (inter-AUG) insertion mutant (FMDV-Mut) (Piccone et al., 2010b) derived from the same parental virus. The data herein demonstrate that the pathogenesis of FMDV-WT was similar to FMDV-O_1-Manisa with primary replication in nasopharynx followed by extensive amplification in the lungs followed by viremia and clinical disease. By contrast, FMDV-Mut had a thoroughly attenuated phenotype (when inoculated via aerosol) which was associated with lower levels of replication at primary sites and lung, lack of detectable viremia and no clinical signs. The differences between the two viruses were associated with significant divergence in induction of type I/III IFN both locally and systemically. Interestingly, inoculation of FMDV-Mut via intraepithelial lingual injection restored fully virulent phenotype and associated IFN response. These data indicate that the virulence of FMDV is dependent upon a delicate balance of intrinsic viral qualities, host defense mechanisms, and route of exposure.

Results

Clinical signs, systemic viral dynamics, and systemic interferon activity (aerosol inoculated cattle)

In cattle aerosol-inoculated with FMDV-WT, the period 24–72 hpa corresponded to the transition from incubation period to early clinical disease (Fig. 1A). At 24 hpa, animals had no clinical signs of FMD and infectious FMDV was not detected in serum; however, low quantity of vRNA was detected in the serum in 71% of animals ($n=7$) with mean GCN$=4.02\pm0.36$/ml and in nasal or oral secretions of all animals (mean GCN$=4.80\pm0.38$ oral; 6.57 ± 0.38 nasal). This vRNA indicated *de novo* FMDV replication rather than residual inoculum, based upon extinction of detection of vRNA (inoculum) in samples obtained from 0 -6 hpa (data not shown). All steers inoculated with FMDV-WT had infectious virus (determined by VI) in nasal secretions at 24 hpa (data not shown).

At 48 hpa three of four steers had one or more vesicle (s) indicating the onset of clinical FMD. All steers were viremic (mean serum GCN$=6.27\pm0.20$/ml; 4/4 VI positive). Oral and nasal secretions were generally VI-positive with similar or higher quantities of vRNA (mean GCN$=5.77\pm1.22$ oral; 7.86 ± 0.53

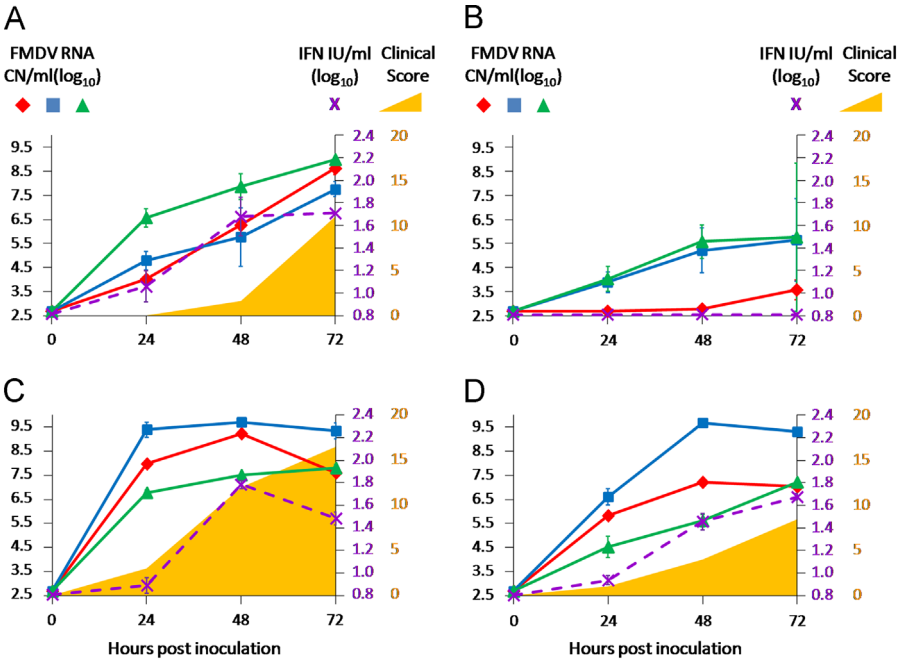

Fig. 1. Graphs illustrating the antemortem dynamics of FMDV infection in cattle: aerosol inoculation with FMDV-WT (A) or FMDV-Mut (B); intra-epithelial lingual inoculation with FMDV-WT (C) or FMDV-Mut (D). Time on the *X*-axes is in hours post-inoculation. The left *Y*-axes represent $\log_{10}$ RNA copy numbers per ml of virus in serum (♦), oral swabs (■) and nasal swabs (▲). The right *Y*-axes represent $\log_{10}$ IFN IU per ml in serum (*X*) and clinical score (shaded area).

nasal) compared to 24 hpa. At the final time point, 72 hpa, both steers had increased clinical lesion scores and vRNA detection from every clinical sample type relative to 48 hpa (mean GCN: serum = 8.63 ± 0.26/ml, saliva = 7.75 ± 0.31/ml, nasal = 9.00 ± 0.09/ml). All sera and secretions from FMDV-WT-aerosolized animals were VI-positive at 72 hpa (data not shown).

In contrast to animals infected with FMDV-WT, none of the six steers aerosol-inoculated with FMDV-Mut had clinical signs of FMD (Fig. 1B) during the 72 hpa described herein. FMDV-Mut infectious virus was never isolated from sera of infected animals; however small quantities of vRNA were detected between 48–72 hpa. Mean vRNA detected in sera was significantly less in FMDV-Mut aerosol-inoculated steers compared to steers aerosolized with FMDV-WT at all time points (24 hpa $p = 0.0056$; 48 hpa $p < 0.0001$; 72 hpa $p = 0.0092$). vRNA and infectious FMDV-Mut were variably detected in nasal and oral secretions with consistently increasing quantities over the 24–72 hpa period, but at uniformly lower quantities compared to animals infected with FMDV-WT at similar time points (Fig. 1A and B). Mean vRNA detected in saliva was significantly less in FMDV-Mut aerosol-inoculated steers at 48 hpa ($p = 0.0496$); mean vRNA detected in nasal swabs was significantly less in FMDV-Mut aerosol-inoculated steers at 24 hpa ($p = 0.0022$) and 48 hpa ($p = 0.0404$).

Systemic type I/III interferon activity was investigated in time-dependent manner in sera from aerosol and IEL-inoculated steers (described below). Cattle that were aerosol-inoculated with FMDV-WT had a robust and consistent type I/III IFN activity in serum (Fig. 1A). Induction of IFN activity was regularly first detected in serum between 24–48 hpa and always occurred coincident with detection of vRNA in serum. At 48 hpa all animals had elevated activity and maximum levels were detected between 48–72 hpa. The highest single measurement of IFN activity in serum (128.75 IU/ml) occurred at 48 hpa. Serum detection of IFN activity was similar between 48 and 72 hpa in contrast to detection of vRNA in serum, which increased by more than 2 $\log_{10}$ in the same time period. By contrast, steers aerosol-inoculated with FMDV-Mut did not have detectable levels of type I/III IFN in serum at any time (Fig. 1B); systemic IFN activity was statistically significantly higher amongst FMDV-WT-inoculated steers at 48 and 72 hpa.

Clinical signs, systemic viral dynamics, and systemic interferon activity (intra-epithelial lingual inoculated cattle)

In order to investigate inoculation route-dependence of clinical phenotype, viral dynamics, and systemic type I/III interferon response of cattle inoculated with FMDV-WT and FMDV-Mut, two steers were inoculated with each virus by conventional intra-epithelial lingual injection and monitored similarly as described for aerosol-inoculated cattle (Fig. 1C and D). The most striking difference observed in these experiments was that FMDV-Mut had a virulent phenotype when inoculated IEL (Fig. 1D). In order to investigate if this regained virulence was due to genomic alterations of FMDV-Mut, full length Sanger sequencing of the entire FMDV open reading frame was performed on vesicular fluid from the earliest vesicles observed in each of the IEL-inoculated steers. Sequencing confirmed that the inter-AUG transposon was intact and that no compensatory mutations had occurred anywhere in the open reading frame relative to the inoculated virus (data not shown). Both steers inoculated with this virus by this route had clinical signs of FMD including fever and vesicles at the injection site and distant secondary sites (feet). Viremia and viral shedding were also consistent with the dynamics of virulent FMDV with maximum detection of vRNA in serum at 48 hpi (7.22 ± 0.11 RNA/ml) and maximum shedding in nasal secretions at 72 hpi (7.22 ± 0.03 RNA/ml).

Although, these data clearly indicate reconstitution of virulence in association with IEL inoculation, FMDV-Mut was still relatively attenuated when compared to FMDV-WT inoculated IEL at the same dose (Fig. 1C). Within the same 72 hpi monitoring period, maximum clinical lesion score was significantly higher ($p = 0.0337$) for FMDV-WT infected steers (16.5 ± 0.88) as compared to FMDV-Mut (8.50 ± 1.94). Similarly, IEL inoculated FMDV-WT achieved significantly higher maximum vRNA detections in serum (9.24 ± 0.05 RNA/ml; $p = 0.0018$) and in nasal secretion (7.81 ± 0.16 RNA/ml; $p = 0.0529$) compared to FMDV-Mut (serum: 7.22 ± 0.11 RNA/ml; nasal: 7.22 + 0.12 RNA/ml). Systemic IFN activity was substantial, but not significantly different, in IEL-inoculated animals with either virus (Fig. 1C and D): FMDV-WT (max 62.55 ± 4.82 U) and FMDV-Mut (max 48.11 ± 3.01 U). Similar to animals aerosol-inoculated with FMDV-WT, IFN activity correlated closely with detection of vRNA in

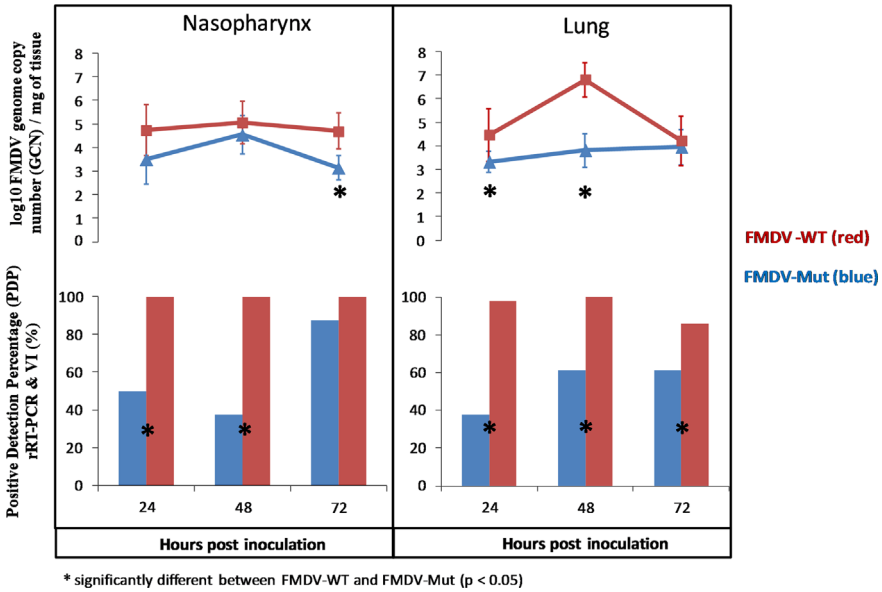

Fig. 2. Tissue-specific, timepoint-specific comparison of FMDV detection by Genome Copy Numbers and Positive Detection Prevalence (PDP) in tissues of cattle aerosol-inoculated with either FMDV-WT or FMDV-Mut.

serum. Thus, FMDV-Mut induced viremia, systemic FMD, and a systemic (responsive) IFN response when delivered via the IEL route.

Tissue-specific distribution of FMDV and viral RNA in aerosol-inoculated steers

In order to compare differences in tissue-specific viral loads due to factors directly attributable to the inter-AUG mutation, two parameters were defined and compared across FMDV-WT and FMDV-Mut. The first parameter was mean genome copy number (GCN) which was calculated from all FMDV rRT-PCR replicates from each anatomically defined tissue from all animals infected with the same virus and euthanized at each particular time point. The second parameter was tissue-specific FMDV positive detection prevalence (PDP), similarly calculated for all animals infected with the same virus and euthanized at the same time point.

At all time points and all tissues examined, both GCN and PDP were higher for tissues of animals infected with FMDV-WT as compared to tissues from animals infected with FMDV-Mut, indicating a substantially higher viral load in tissues of animals infected with FMDV-WT (Fig. 2). GCN was significantly higher ($p < 0.05$) for nasopharyngeal tissues at 72 hpa and for lung tissues at 24 and 48 hpa. The greatest difference in GCN between FMDV-WT and FMDV-Mut and lowest p-value for statistical significance occurred for lung tissues at 48 hpa. PDP was significantly higher ($p < 0.05$) for all tissue/time point combinations except for nasopharyngeal tissues at 72 hpa ($p = 0.3192$). The greatest difference in PDP and lowest p-value for statistical significance occurred for lung tissues at 24 hpa (Fig. 2).

Tissue-specific type I/III IFN activity and transcription of IFN and ISG

Mean relative induction (or repression) of transcription of IFN and ISG was characterized in various tissues of cattle aerosolized with FMDV-WT and FMDV-Mut (Fig. 3). Multiple tissue replicates from multiple animals were included for every time point. On the basis of previous work delineating specific roles for distinct anatomic regions in FMD pathogenesis (Arzt et al., 2010; Pacheco et al., 2010a; Zhu et al., 2013), tissues were grouped into the categories: primary infection sites (nasopharynx), intermediate infection sites (lung) and lesion predilection sites (tongue epithelium and interdigital skin). Mean fold-changes of transcription induction were compared between tissues of animals infected with FMDV-WT and FMDV-Mut.

At the local tissue level, the general trend was that transcription of IFN-α, IFN-β, and IFN-λ were substantially induced (up to 2482-fold) in lung and lesion predilection site tissues of both FMDV-WT and FMDV-Mut aerosolized animals with no significant difference between the effects of the two viruses (Fig. 3). Despite similar induction of IFN transcription, ISG mRNAs had nearly uniformly higher induction amongst FMDV-WT infected cattle with significant findings in every tissue class and every time point. The overall trend of IFN/ISG transcription induction is particularly well exemplified by the lesion site tissues at 72 hpa wherein IFN-α, IFN-β, and IFN-λ transcription were similarly highly induced amongst both virus groups; however, ISG transcription induction was significantly higher within tissues of FMDV-WT infected steers for all ISGs except IRF-7 (Fig. 3).

In nasopharyngeal tissues, IFN mRNAs were modestly induced to moderately suppressed for both viruses with only a single significant finding of IFN-λ being suppressed more in FMDV-WT infected animals at 72 hpa. Despite similar (i.e. not significantly different) changes in IFN mRNAs, there were numerous significant differences in relative induction of ISG mRNA between animals infected with the two viruses. Significantly different mean inductions of ISGs were identified in all tissue categories and included the mRNAs coding for IRF-7, CCL-2, OAS, PKR, and Mx-1 (Fig. 3); in every case of significant difference, the mean ISG induction was

			Host mRNA										IFN-Bioactivity (IU/g)	FMDV vRNA GCN/mg
			IRF-7	CCL-2	OAS	PKR	MX-1	IP-10	iNOS	IFN-a	IFN-b	IFN-λ		
FMDV-WT	24hpa	Nasopharynx‡	16.39	**3.67**	**1.82**	**1.42**	**3.44**	4.15	1.11	0.74	0.52	3.99	**932.7**	**3.83**
		Lung	177.34	0.62	3.95	2.03	6.08	0.51	0.18	2.04	0.85	29.30	**668.7**	**4.94**
		Lesion sites	18.97	0.74	2.58	0.80	**1.67**	0.00	5.34	5.94	0.97	95.22	**Neg**	**Neg**
	48hpa	Nasopharynx	10.34	2.24	**2.61**	**1.50**	2.94	3.50	0.52	2.94	0.79	3.12	**710.7**	**3.46**
		Lung	117.94	0.95	5.85	2.24	3.83	1.51	**0.05**	6.75	2.93	1928.71	**4341.0**	**6.28**
		Lesion sites	22.67	1.26	**11.81**	**2.03**	**5.36**	1.20	0.59	919.68	17.42	264.10	**Neg**	**Neg**
	72hpa	Nasopharynx	**0.04**	4.08	**1.77**	**1.34**	**2.20**	2.46	0.84	0.13	0.27	**0.10**	**Neg**	**3.45**
		Lung	1.00	1.00	3.60	1.48	6.87	0.86	0.17	30.00	7.57	70.68	**671.1**	**4.22**
		Lesion sites	2.21	**69.22**	**31.71**	**4.83**	**21.38**	**52.67**	**186.50**	1114.91	71.50	2482.87	**6762.0**	**8.05**
FMDV-Mut	24hpa	Nasopharynx	3.66	**0.57**	**0.26**	**0.30**	**0.64**	0.26	0.74	3.93	0.57	1.51	**Neg**	**3.62**
		Lung	12.84	0.33	1.79	1.70	3.16	0.34	0.43	916.89	14.52	769.61	**Neg**	**4.37**
		Lesion sites	9.27	0.71	0.44	0.28	**0.97**	0.25	2.58	1903.47	33.59	642.84	**Neg**	**Neg**
	48hpa	Nasopharynx	6.01	1.34	**0.43**	**0.40**	0.80	0.28	0.62	2.51	0.82	2.54	**Neg**	**2.83**
		Lung	62.48	0.38	1.70	1.42	2.13	0.52	**0.26**	237.33	5.98	398.42	**Neg**	**3.84**
		Lesion sites	15.97	2.48	**1.16**	**0.29**	**0.78**	6.95	0.73	1517.20	95.81	1555.91	**Neg**	**Neg**
	72hpa	Nasopharynx	**0.01**	1.06	**0.34**	**0.42**	**0.50**	0.48	0.78	0.78	0.59	**0.59**	**Neg**	**3.64**
		Lung	0.42	0.28	1.39	0.64	1.24	0.08	0.14	556.03	4.90	554.17	**Neg**	**3.63**
		Lesion sites	2.05	**1.50**	**1.35**	**0.24**	**0.76**	**0.00**	**0.00**	1048.66	99.79	2431.21	**414.9**	**Neg**

Color coding of fold changes						
<0.01	0.01-0.1	0.1-1	1-10	10-100	100-1000	>1000

*Each data point (i.e. cell) is the mean relative induction (fold-change) for all tissues in that anatomic category from animals infected with that virus and euthanized at that time. Fold-change was calculated by ΔΔCt method of Pfaffl using baseline expression calculated from 3 mock-inoculated steers. **Bold underlined** font indicates significantly greater/lesser detection when compared across virus (FMDV-WT vs. FMDV-Mut).

‡Nasopharynx tissues include dorsal soft palate and dorsal nasopharynx. Lesion site tissues include tongue and interdigital skin.

Fig. 3. Comparison of relative induction of transcription of type I/III interferons and interferon-stimulated genes in tissues obtained from cattle aerosol-infected with FMDV-WT or FMDV-Mut*.

higher amongst FMDV-WT infected animals compared to FMDV-Mut. It is also noteworthy that both viruses, most noticeably FMDV-Mut, induced transcription of IRF-7 in all tissues between 24–48 hpa, but nearly uniformly downregulated its transcription at 72 hpa as viral titers increased.

Both viruses effectively induced IFN transcription at lesion predilection sites. Remarkably this was the case for FMDV-Mut-infected animals despite lack of detection of FMD infectious virus or RNA at such sites. However, ISG induction was only seen in animals infected with FMDV-WT wherein virus and IFN activity were detected at these sites.

Several tissues from FMDV-WT-infected cattle had detectable type I/III IFN bioactivity (Fig. 3). It is noteworthy that detection of IFN activity in tissues was generally one order of magnitude higher than that detected in serum when comparison was made using units of similar mass (i.e. IFN IU/ml for serum and IFN IU/g for tissue). At 24 hpa, one nasopharyngeal and one lung tissue had bioactivity of 932.7 IU/g and 688.7 IU/g respectively. At 48 hpa, maximum IFN detection in nasopharyngeal tissue had decreased to 710.7 IU/g; however, in lungs, coincident with maximum vRNA detection, IFN bioactivity reached 4341.0 IU/g, representing the peak of pulmonary IFN detection. At 72 hpa, the highest tissue-specific level of IFN

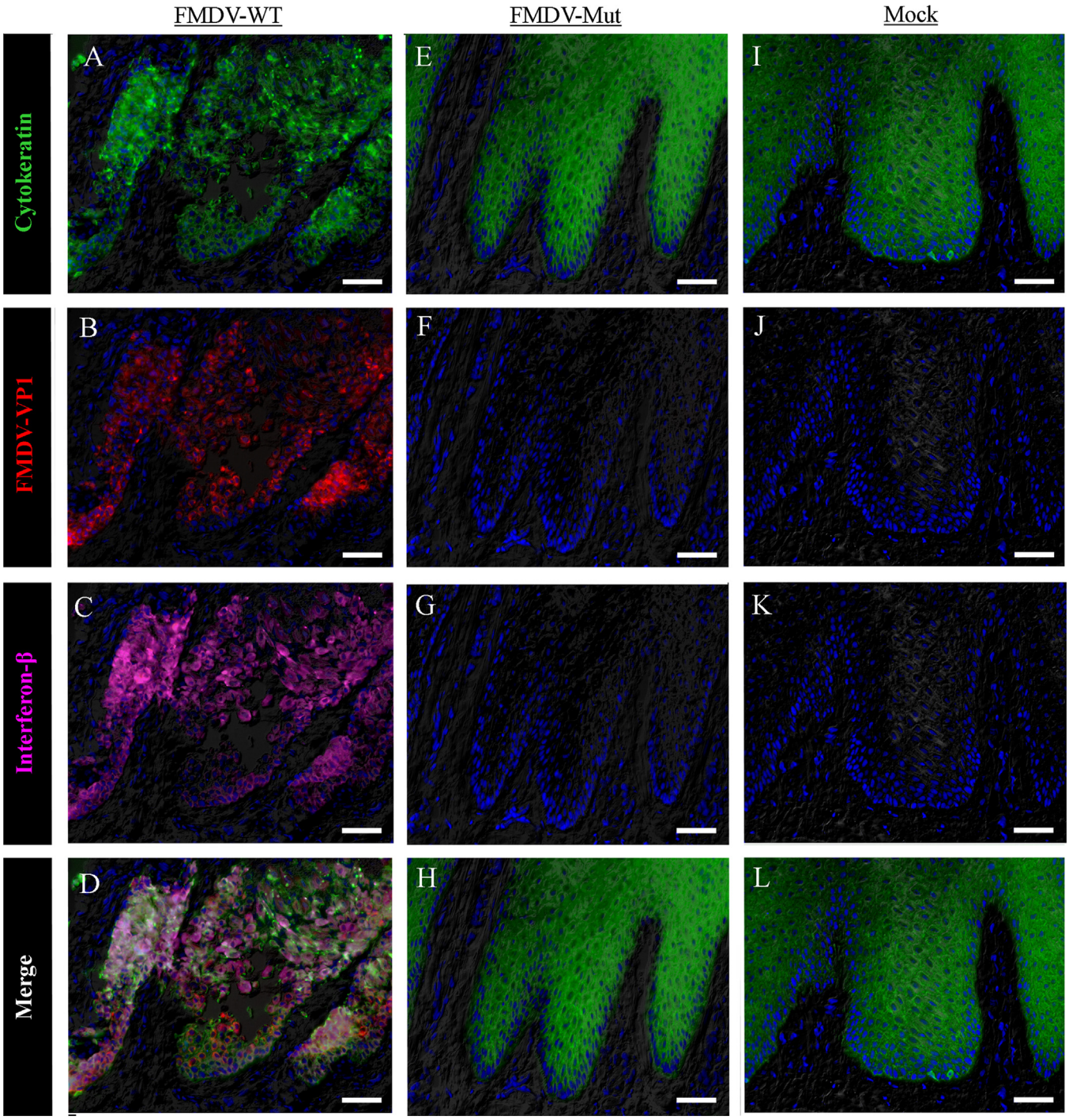

Fig. 4. Immunofluorescent labeling of interdigital epithelium from cattle aerosol-inoculated with FMDV-WT (A–D), FMDV-Mut (E–H), or virus-free media (Mock, I–L). A regionally extensive vesicle cavity in FMDV-WT tissue is comprised of numerous cells containing cytokeratin, FMDV-VP1, and IFN-β. Mock and FMDV-Mut derived tissues lack FMDV-VP1 and IFN-β staining. Simultaneous multichannel indirect immunofluorescent technique, hematoxylin counterstain, 20 ×, bar = 50 μ.

bioactivity throughout the study (6762 IU/g) was detected from the lesion predilection tissue category (i.e. tongue epithelium), coinciding with high levels of vRNA and vesicle formation. At this time, IFN detection from lungs had decreased to 671 IU/g, and nasopharyngeal tissues had no detectable IFN. The only IFN bioactivity detected in any tissue from cattle inoculated by aerosol with FMDV-Mut occurred in tongue epithelium at 72 hpa in the absence of any clinical signs; this bioactivity of 414.9 IU/g was lower than any IFN activity detected for FMDV-WT. (Fig. 3)

Microscopic characterization of animal tissues of aerosol-inoculated cattle

With the exception of gross lesion sites, histological characteristics and microanatomic localization of FMDV antigens were remarkably similar regardless of the virus (FMDV-WT or FMDV-Mut) with which cattle were aerosol-inoculated (not shown). Both viruses were first localized within the epithelia of MALT regions of nasopharynx at 24 hpa. At 48–72 hpa both viruses could be localized to lungs of infected cattle; however, cattle infected with FMDV-WT had substantially greater quantities of lung specimens containing virus antigen and positive tissues generally had more antigen-positive cells compared to samples of lungs from animals infected with the mutant virus.

The most remarkable microscopic difference between cattle infected with the two viruses was the cavitary intraepithelial vesiculation present at multiple pedal and oral epithelial lesion sites, only of cattle infected with FMDV-WT (Fig. 4). Multichannel immunofluorescent microscopy indicated that the lesions were comprised of degenerating cytokeratin-positive cells (keratinocytes), many of which were immunoreactive for FMDV-VP1 and/or IFN-β. Few MHC-II containing cells were present within lesions; however these cells uniformly lacked immunoreactivity for FMDV-VP1 and IFN-β (Fig. 5). No vesicles were identified grossly or microscopically in pedal or oral epithelia of FMDV-Mut infected cattle; neither FMDV-VP1 nor IFN-β could be identified microscopically in lesion predilection sites from these animals (Fig. 4).

Discussion

In order to investigate mechanisms of virulence and attenuation of FMDV, experiments were conducted in which cattle were inoculated by a simulated natural route (aerosol) or parenteral injection (IEL) with either a mutagenized FMDV containing a transposon insertion in the inter-AUG region of L_{pro} (FMDV-Mut) or the parental infectious clone (FMDV-WT) from which the mutant virus was derived. Previous work from our laboratory demonstrated that FMDV-WT is virulent and FMDV-Mut is attenuated in cattle by the aerosol route (Piccone et al., 2010b). Furthermore, other than a slower replication rate for FMDV-Mut, previous work found no major differences in basic functions or intracellular localization of FMDV-Mut leader protease and the WT protein (Piccone et al., 2010a). Recent work investigating various deletion mutants of the inter-AUG (spacer) region showed differential L_{pro} function and cell-line specific viability dependent upon what portion of inter-AUG sequence was retained or deleted (Belsham, 2013). This suggests that the inter-AUG region may be critical in determining FMDV tropism and pathogenesis *in vivo*.

The central hypothesis of the current work was that intensive sampling, analysis, and comparison of animals infected with FMDV-WT or FMDV-Mut would reveal host and viral factors that define the nature of virulence of FMDV in cattle. Examination of tissues and clinical samples of animals at 24–72 hpa indicated that inoculation of FMDV-WT as opposed to FMDV-Mut determined substantial differences in tissue-specific virus loads, variations in transcription of several host genes, and distinct patterns of type I/III interferon activity. Although, tissue distribution and microscopic examination indicated some similarities, there were specific differences that were linked to distinct differences in the pathogenesis of the two viruses.

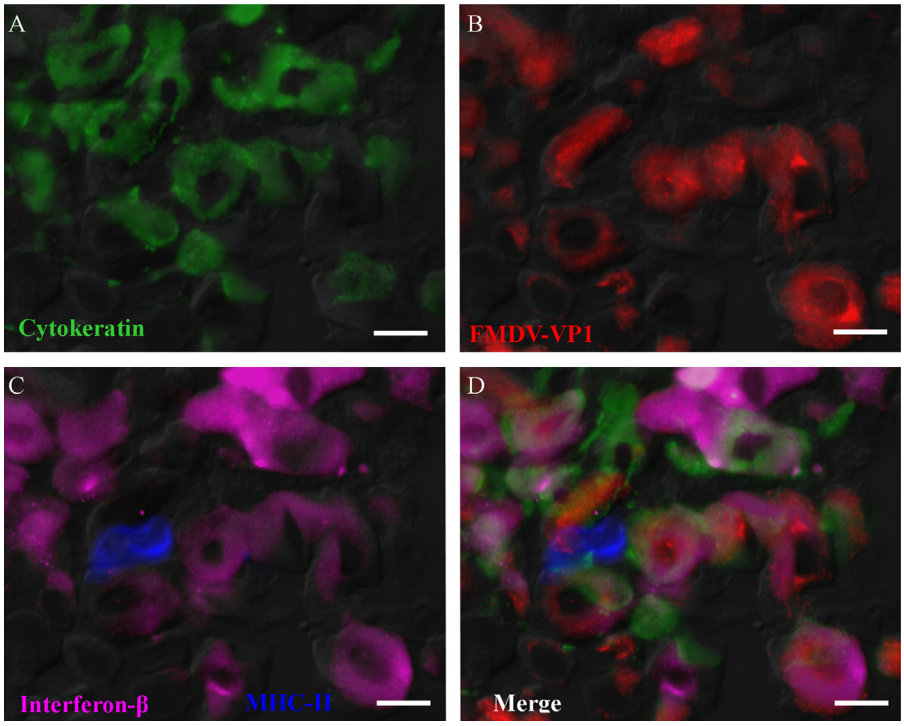

Fig. 5. Center of vesicle, interdigital epithelium, 72 hpa, FMDV-WT. (A) Most cells are keratinocytes that are labeled with anti-cytokeratin (green). (B) Many cells contain FMDV-VP1 (red). (C) Few cells containing MHC-II (blue) are distinct from cells containing IFN-β (purple). (D) Merge indicates variable co-localization of cytokeratin, FMDV-VP1, and IFN-β. Simultaneous multichannel indirect immunofluorescent technique with differential interference contrast, 100×, bar = 10 μ.

The most readily apparent differences between the two viruses were the complete clinical attenuation after aerosol inoculation, failure to establish viremia (infectious virus), and relative inefficiency of replication of FMDV-Mut in various tissues as compared to FMDV-WT. While it is likely that these differences in viral dynamics reflect a combination of viral (intrinsic) and host (extrinsic) factors, the association of high viral loads and virulence is unambiguous in the current study. Both the distribution of virus and the regional viral loads were significantly higher for FMDV-WT as reflected by the PDP and GCN parameters respectively. Relatively low viral loads were apparent at all time points in both antemortem samples and postmortem specimens from steers aerosol-inoculated with FMDV-Mut. The antemortem disparity is demonstrated by the significant differences in maximum recovery of vRNA from serum (5 $\log_{10}$ higher for FMDV-WT), nasal secretions (3 $\log_{10}$ higher for FMDV-WT), and oral secretions (2 $\log_{10}$ higher for FMDV-WT). The disparity in viral loads in tissues was most evident in lungs at 48 hpa (3 $\log_{10}$ higher for FMDV-WT) however the same trend was true for every tissue and every time point examined. Recent work from our laboratory has demonstrated that localization of large quantities of FMDV in pulmonary epithelial cells is a consistent finding in early stages of viremia of FMDV aerosol-inoculated cattle (Arzt et al., 2010). The current association of elevated pulmonary viral loads concurrently with viremia and virulence of FMDV-WT suggests that replication of FMDV in the lungs plays a critical role in virus generalization and clinical disease after infection by aerosol.

The differences in host innate response to the two viruses are complex and require consideration of compartmentalization of effects (local and systemic) and distinct layers of regulation (e.g. transcriptional, translational, post-translational). Since the WT virus induced a more robust systemic and tissue-specific innate response, it cannot be concluded that more efficient induction of IFNs and ISGs is allowed by FMDV-Mut and thus resulted in attenuation. However, it cannot be ruled out that IFN responses elicited prior to 24 hpa may have gone undetected yet contributed to limiting early replication and/or dissemination of the mutant virus. Additionally, it is plausible that the very early virus-host interaction *in vivo* involves just a small number of infected cells in which IFN responses might be differentially affected by the WT and mutant viruses, yet these subtle differences were not detectable by current techniques which assay host innate responses at the macroscopic (i.e. whole tissue) level. Furthermore, it is possible that such IFN-susceptibility of FMDV is an important mechanism within individual cells *in vivo* and that IFN limits viral replication in such cells similarly as has been demonstrated in cell culture (Chinsangaram et al., 2003; Diaz-San Segundo et al., 2011; Moraes et al., 2007).

It is clear that from 0–72 hpa the virulent FMDV-WT thrived despite substantial levels of IFN activity. Peak viremia, highest tissue-specific viral loads and the onset of vesiculation all occur in the context of peak type I/III interferon activity. This is consistent with recent works that have demonstrated that the early phase of FMD in cattle includes coincident peaks of viremia and systemic IFN activity followed by detection of specific antibodies (Howey et al., 2012; Perez-Martin et al., 2012; Stenfeldt et al., 2011). However, experiments in cell culture have shown that successful replication and spread of virulent FMDV required blocking the expression of IFN and ISGs (Chinsangaram et al., 1999; de los Santos et al., 2007). Similarly, in tissue culture experiments in our laboratory, no detectable IFN activity could be detected after infection with FMDV-WT of a primary cell culture generated from embryonic bovine kidney cells, whilst modest activity was detected subsequent to infection of cells with FMDV-Mut (data not shown). These seemingly contradictory findings between cell culture and *in vivo* studies suggest that complex virus-host interactions at very early stages of infection determine the outcome of the infection. Establishment of productive infection (in either system) may depend upon a fine balance between the rate of replication and the timing and extent of induction of IFN and ISG for each particular virus strain.

The current data indicates that during acute FMD peripheral tissues contain substantially more type I IFN than is present within similar mass or volume of blood. The greatest detection in tissues was 6762 IU/g which is more than 50-fold greater than the maximum detection in serum of 129 IU/ml. Additionally, the microscopic co-localization of IFN-β and FMDV antigens in vesicular tissue suggests that infected epithelial cells are a substantial source of type I IFN. Furthermore, co-localization of IFN- β with cytokeratin but not MHC-II suggests that at lesion sites, keratinocytes, but not antigen-presenting cells, are responsible for the regionally detected IFN activity. This finding provides the first scientific evidence for a differential role of infected epithelial cells versus non-infected immune cells as major sources of type I IFN in FMDV infected tissues.

Recent work has demonstrated that *ex vivo* enriched plasmacytoid dendritic cells (pDCs) are a rich source of type I IFN in cattle responding to FMDV, which leads the authors to suggest that these intravascular cells are the major source of type I interferon in response to FMDV *in vivo* (Reid et al., 2011). However, if intravascular pDCs were the major source of IFN, then it would follow that upon examination of individual tissues, type I/III IFN activity would be expected to be ubiquitously present in quantities proportional to the blood content of the tissue. Yet this was not the case in the study described herein. Rather, detection of IFN activity in tissues was highly restricted anatomically and temporally to sites of intense virus replication. This further supports the premise that the tissues where virus replicates are selectively induced to generate large quantities of IFN. The extent to which this IFN enters the vascular space and contributes to detection of IFN in sera remains uncertain, but it is plausible that IFN could gain access to the systemic circulation directly through blood capillaries or via the lymphatic system.

The induction/repression of transcription of IFN and ISG in tissues during FMDV infection provides novel insights to the antiviral mechanisms engaged at these sites. Previous works have demonstrated IFN induction in PBMCs at 1dpi (Perez-Martin et al., 2012), in NALT at 7dpi (Zhang et al., 2006), in various epithelia at 1–4dpi (Zhang et al., 2009) and repression in nasopharynx biopsies at onset of the acute phase (Stenfeldt et al., 2012). The general trend herein that ISG were upregulated and IFN activity induced more in tissues from FMDV-WT infected steers further supports the concept that a more robust antiviral response was occurring in these animals at the time points examined herein. Furthermore this data suggests that within infected tissues of cattle, virulent FMDV induces interferon pathways rather than suppresses the innate response. The inhibition of IFN response observed *in vitro* in FMDV infected cells might still be occurring at the individual cell level, but was not detectable *in vivo* at the whole tissue level.

The elevated tissue-specific transcription levels of OAS, PKR, Mx-1, IRF-7, and IP-10 (Fig. 3) provide a temporo-anatomic map of which specific pathways may have been activated. This is consistent with previous works that describe such ISG-expression patterns associated with type I/III IFN activity (Sadler and Williams, 2008; Sommereyns et al., 2008). The clearest example of antiviral activation occurred in the lesion predilection site tissues of FMDV-WT infected steers wherein IFN-α, β, and λ were all induced, maximum IFN bioactivity was detected, and 6 of 7 ISGs were significantly upregulated relative to FMDV-Mut. An intriguing quandary is that IFN mRNAs were similarly upregulated in various tissues (including lesion predilection sites) of FMDV-Mut infected animals despite lack of detectable lesions, FMDV, IFN activity, or ISG induction. The disconnect between

induction of type I/III IFN mRNA and IFN activity or ISG induction at lesion target sites in these animals is suggestive of activation of a generalized (primary) IFN signal induced by the FMDV-Mut infection of primary sites, but lack of a (secondary) IFN inducing signal such as viral RNA at target sites (i.e. viremia). This is consistent with similar work from our laboratory demonstrating up-regulation of ISGs after infection with FMDV-WT prior to viremia and manifestation of systemic disease (Diaz-San Segundo et al., 2010). The mechanism of this activation of IFN mRNA at lesions sites remains unclear; however, it is possible that the low levels of FMDV-Mut vRNA detected in sera, but below the limit of local detection in tissues, were involved in this distant transcription induction of IFN genes.

The fact that FMDV-Mut was virulent when inoculated directly in the epithelium of the tongue is suggestive of possible mechanisms that mediated its attenuation under the simulated natural (i.e. aerosol) inoculation route. A complex of inter-related mechanisms, likely, contributed to the reconstitution of virulence of FMDV-Mut upon IEL-inoculation. Virus inoculated via aerosol encounters various innate immune mechanisms in the early stages of infection. These include the intact physical epithelial barrier, the mucocilliary apparatus, dilution effect of secretions, and antimicrobial peptides such as defensins. Additionally, aerosol-inoculated virus initially has very limited replication at minute foci within the nasopharynx (Arzt et al., 2010). By contrast, IEL (needle) inoculation bypasses these host barriers and defense mechanisms. Furthermore, with IEL inoculation, FMDV immediately encounters a population of cells (keratin-rich, αV-integrin-rich epithelial cells) which are known to be exquisitely susceptible to infection and high-titer replication which boosts the effective inoculation dose even higher.

It is possible that virulent phenotype is a direct consequence of the stochastic effect of a larger bolus of FMDV-Mut delivered at a susceptible single site versus the same amount of virus spread over a large surface of the respiratory tract. The overall effect was that the advantages conferred by IEL inoculation (as compared to aerosol) allowed even the intrinsically semi-competent virus to produce a fully virulent phenotype. However, the failure of the IEL inoculated FMDV-Mut to reach the clinical scores and viral loads of the IEL inoculated FMDV-WT during similar time points post-infection further demonstrates the intrinsic limitations of the mutant virus.

The current work challenges the concept that virulence or attenuation of FMDV is determined predominantly by the virus's relative ability to inhibit IFN pathways. Rather, at the early stages of infection, the intrinsic viral properties that define replicative competence may be the most important determinants of virulence. Specifically, after simulated natural inoculation, an attenuated virus actually induced a weaker innate response than the virulent parental virus. At the time points examined herein, prolific replication of the virulent virus has occurred despite the robust innate immune response. These results add complexity to our previous observations which demonstrated that FMDV is susceptible to the antiviral effect of type I/III IFNs and support the concept that a fine balance exists between viral proliferation and host innate immunity. Deeper understanding of these factors defining balance between virulence and attenuation will ultimately be useful in devising better preventive tools such as vaccines and biotherapeutics targeting the critical early steps in FMDV infection.

Materials and methods

Experimental animals, viruses, and inoculation systems

Twenty Holstein steers 9–12 months old, weighing 300–450 kg were obtained from an AAALAC-accredited experimental-livestock provider (Thomas-Morris Inc., Reisterstown, MD). All experiments involving live animals were performed under an experimental protocol approved by the Institutional Animal Care and Use Committee of the Plum Island Animal Disease Center. For all experiments, animals were housed individually in a BSL-3 animal facility from time of inoculation until time of euthanasia. Thirteen steers were inoculated with FMDV via aerosolization (described below) of inoculum (7 with FMDV-WT; 6 with FMDV-Mut) and subsequently euthanized at predetermined end points at 24 h post aerosol inoculation (hpa), 48 hpa, or 72 hpa (Table 1). Four steers were inoculated by conventional intra-epithelial lingual (IEL) inoculation (Henderson, 1949) with FMDV (2 with FMDV-WT; 2 with FMDV-Mut). These IEL inoculated animals were allowed to survive through the acute phase of FMD. Three steers were aerosol inoculated with virus-free media and euthanized 72 hpa for the purpose of recovering tissues for establishing baseline levels of cytokine mRNA.

The "wild type" FMDV utilized in experiments herein (FMDV-WT) is an infectious clone virus of a field isolate of FMDV-A_{24}-Cruzeiro (Rieder et al., 2005); the inter-AUG mutant described herein (FMDV-Mut) was previously described and referred to as "A24-L1123" (Piccone et al., 2010b). Briefly, FMDV-Mut contains a random, 57 nucleotide, in-frame insertion in the region located between the two functional AUG (inter-AUG), within the leader protease (Lpro).Virus inoculum for aerosol and IEL inoculations consisted of 10^7 $TCID_{50}$ FMDV in 2.0 and 0.4 ml, respectively of Minimum Essential Media (Gibco, San Diego, CA) with 25 mM Hepes (Gibco, San Diego, CA).

Steers were sedated with xylazine for all inoculations. Briefly, for aerosol inoculation, each steer was fitted with a commercially available aerosol delivery system (Aeromask-ES, Trudell Medical, London, Ontario, Canada) which was placed over the muzzle (Pacheco et al., 2010a). The mask was attached to a jet nebulizer (Whisper Jet, Vital Signs Inc., Totowa, NJ) which was subsequently attached to an air compressor which generated 25 psi of pressure. Aerosolization proceeded until the complete inoculum was expelled from the nebulizer cup (10–15 min). The same dose of the same stock viruses was delivered by IEL inoculation to similarly sedated steers as previously described (Pacheco et al., 2010a). Clinical scores were based on a 20 point scale accounting for presence of vesicles on each foot and anywhere on head (oral cavity or nasal epithelia) as previously described (Pacheco et al., 2010a).

Sample collection

Antemortem sampling consisted of collection of whole blood in serum separation tubes, and undiluted oral and nasal fluids with

Table 1
Assignment of steers to experimental groups.

	Virus used		
	FMDV-WT	FMDV-Mut	None (mock)
Route/time			
Aer[a]/24 hpa	$n=3_{v,t,i,h}$	$n=2_{v,t,i,h}$	N/A
Aer/48 hpa	$n=2_{v,t,i,h}$	$n=2_{v,t,i,h}$	N/A
Aer/72 hpa	$n=2_{v,t,i,h}$	$n=2_{v,t,i,h}$	$n=3_b$
IEL[b]/10dpi	$n=2_{v,i}$	$n=2_{v,i}$	N/A

Subscripts indicating animals' usage.
v=virus dynamics (antemortem)
t=virus tissue loads (postmortem)
i=IFN activity (antemortem)
h=host tissue-specific mRNA and IFN activity (postmortem)
b=baseline host mRNA

[a] Aer=aerosol inoculation.
[b] IEL=intra-epithelial lingual inoculation.

cotton swabs. All animals were sampled prior to inoculation to ensure FMDV – free status and lack of elevated IFN levels that might interfere with initial FMDV replication. Animals were additionally sampled at several time points throughout the duration of the experiment which varied according to goals of the individual experiments. Swabs and serum tubes were transported from the animal room to the laboratory on ice and were immediately centrifuged for harvesting of serum, saliva, and nasal secretion. Samples were then stored at −70 °C until time of processing.

Steers were euthanized at predetermined time points regardless of clinical progression of disease in individual animals. Postmortem sample collection schemes were predetermined and standardized with minor variation among individual animals based upon the expected stage of disease at the time of euthanasia. Necropsies were performed immediately subsequent to euthanasia. Detailed descriptions of tissue designations and collection strategies has been published previously (Pacheco et al., 2010a). For the current study, tissues analyzed were nasopharynx (8 distinct specimens per animal from dorsal soft palate and roof of nasopharynx), lung (18 distinct specimens per animal from different levels of lung), and lesion predilection sites (up to 12 distinct specimens from dental pad, tongue and foot epithelium).

For each anatomically defined specimen, three 30–50 mg tissue samples were aliquoted into separate screw-cap 1.5 ml tubes and frozen immediately in liquid nitrogen for transfer within 2 h to a −70 °C freezer in which they were stored until the time of processing. An adjacent specimen from each tissue was placed in a cryomold, embedded in Optimal Cutting Temperature Compound (OCT) (Sakura Finetek, Torrance, CA), frozen on a bath of liquid nitrogen, and stored at –70 °C for immunomicroscopy.

Foot-and-mouth disease vRNA detection

For tissues, two samples of each specimen were thawed and immediately macerated in a TissueLyser bead beater (Qiagen, Valencia, CA) as previously described (Pacheco et al., 2010a). RNA was extracted using Ambion's MagMax-96 Viral RNA Isolation Kit (Ambion, Austin, TX) on a King Fisher-96 Magnetic Particle Processor (Thermo Scientific, Waltham, MA). Once extracted, vRNA was detected by real-time reverse transcription polymerase chain reaction (rRT-PCR) on the ABI 7000 system (Applied Biosystems, Austin, TX) as previously described (Callahan et al., 2002). Samples with cycle threshold (Ct) values <40 were considered positive. Antemortem samples (serum and swabs) were processed similarly with the exception that a single extraction was performed on each sample and subsequently used for 2 replicate rRT-PCR reactions.

Foot-and-mouth disease virus isolation

Virus isolation (VI) was performed separately on the duplicate samples of each tissue on BHK-21 cells as previously described (Pacheco et al., 2010b). Subsequent to evaluation of cytopathic effect (CPE), FMDV-positivity/negativity was confirmed by rRT-PCR on cell culture supernatants. Samples which had no CPE, but from which vRNA was detected by rRT-PCR were passed a second time in BHK-21 cells.

Host IFN and ISG mRNA detection and analyses

In order to establish baseline expression of host genes, 30–50 mg of tissue specimens were individually lysed by adding 600 μl of RLT lysis buffer (Qiagen, Valencia, CA) and macerating using the rotor-stator method. Approximately 600 μl of homogenate was transferred to a Qiagen Qiashredder (Qiagen), and total RNA was subsequently isolated using an RNeasy kit (Qiagen) as recommended by the manufacturer. RNA concentrations were determined using a NanoDrop ND-1000 spectrophotometer. 1.0 μg of RNA was treated with DNase I per manufacturer's instructions (Sigma, St. Louis, MO.) and total RNA was reverse transcribed into cDNA using random hexamers (Thermo Scientific Hanover Park, IL.) per manufacturer's instructions. Samples were thermocycled at 25 °C, for 10 min, 37 °C for 60 min, and 95 °C for 5 min. The cDNA was then diluted with distilled water 1:8 in a final volume of 200 μl.

Baseline levels of expression of 10 host genes of interest were established from individual tissues of mock-inoculated steers ($n=3$) by rPCR systems as previously described (Diaz-San Segundo et al., 2011; Muller-Doblies et al., 2002; Taubert et al., 2006). cDNA was run in triplicate and averaged for each individual specimen. The triplicate averages of the 3 steers were then averaged to generate the negative control baseline Ct for each tissue for all 11 genes of interest. cDNA rPCR was carried out in 25 μL reactions on the ABI 7000 Sequence Detection System using Taqman Universal PCR Master Mix (Applied Biosystems, Foster City, CA.). Samples were thermocycled at 50 °C for 2 min, 95 °C for 10 min, and 40 cycles of 95 °C for 15 s and 60 °C for 60 s.

Experimental tissues (i.e. from FMDV-infected steers) were collected, processed, and analyzed for expression of the 11 genes of interest as described above with the exception that tissues were homogenized in 600 μL of Minimum Essential Media (Gibco, San Diego, CA) to allow for further down-stream processing for interferon type I/III activity detection (described below). The relative mRNA gene expression for tissues of FMDV-inoculated animals was calculated by comparison to the tissue-specific, 3-steer negative control baseline data (generated above) using the previously described ΔΔCt method (Pfaffl, 2001). The Pfaffl method determines the relative expression of the target gene in comparison to a reference gene for which glyceraldehyde-3-phosphate dehydrogenase (GAPDH) was used. This relative quantification was then compared to the baseline levels of expression (ΔCt relative to GAPDH) to generate the fold-change of expression amongst infected animals as compared to uninfected (i.e. baseline). The individual tissue fold-changes were averaged across virus-specific, anatomic-specific, and timepoint-specific categories to generate the tissue specific means presented herein. "Nasopharynx" fold-changes represent the mean of the individual fold-changes determined for all dorsal soft palate and dorsal nasopharynx tissues at each time-point (6 distinct tissues per time point). Similarly, "Lung" is the mean of all fold changes for individual tissues from various level of lung (2 distinct tissues per time point) whilst "Lesion Sites" represents the mean of all values from tongue and interdigital cleft epithelium (4 distinct tissues per time point). For the final output, the mean fold changes were compared by student's *t*-test across the variable "inoculation virus used" to determine if there was significant difference in expression of a given cytokine, anatomic site, timepoint combination based solely upon infection with FMDV-WT vs. FMDV-Mut.

Quantification of type I/III interferon in sera and tissues

An MxA protein chloramphenicol Acetyltransferase (Mx-CAT) reporter gene assay was used to quantitate interferon activity in serum and tissue macerate samples as previously described (Fray et al., 2001). For each assay Madin-Darby bovine kidney-t2 (MDBK-t2) cells, stably transfected with a plasmid containing a human MxA promoter driving a chloramphenicol acetyltransferase cDNA, were plated at a density of 2×10^4 per well in 24 well plates. After 18–20 h of incubation at 37 °C, 5% CO_2, the monolayer was rinsed with serum-free media and replaced with 150 μl/well of Dulbecco's Modified Eagle Medium with 1% FBS, 10 μg of blasticidin/ml culture medium and 100 μl of sample or recombinant

human IFN-α 2a protein standard (PBL Biomedical labs). Plates were incubated for 22–24 h at 37 °C in 5.0% CO_2.

The following day CAT expression was determined using a commercial ELISA kit (Roche Diagnostics) following the manufacturer's instructions. In brief, cells were lysed for 30 min with Triton X-100 lysis buffer and 200-μL aliquots were added in duplicate to wells of the CAT-ELISA 96-well plate. A standard curve was generated in units of international units per ml (IU/ml) from twofold serial dilutions of recombinant human IFN-α 2a (PBL Biomedical labs). The interferon levels of the unknown samples were calculated by extrapolation from the standard curve run on the same day using the same MDBK-t2 cells. For tissue samples, IU/g was calculated based upon the dilution of original tissue in media.

Quantitative analyses of FMDV in bovine tissues and fluids

Ct values generated by FMDV rRT-PCR from experimental specimens were converted to FMDV RNA genome copies per mg as previously described (Arzt et al., 2010). The Ct positivity cutoff for tissues of 40 corresponded to a detection threshold value of 2.52 $\log_{10}$ FMDV RNA copies/mg (RNA/mg) of tissue. FMDV rRT-PCR results were expressed as the mean $\log_{10}$ FMDV RNA copies/mg (RNA/mg) for all anatomically similar tissues from animals infected with the same virus and sampled at each time point. Similarly, for antemortem samples (sera/swabs), data herein represents the mean $\log_{10}$ FMDV RNA copies/ml (RNA/ml) from all animals infected with the same virus and sampled at each time point. The Ct positivity cutoff of 45 corresponded to a detection threshold value of 2.69 $\log_{10}$ FMDV RNA copies per ml of serum or swab sample.

Tissue specific viral loads were further analyzed by defining two parameters as follows. For each anatomically defined tissue, the mean genome copy number (GCN) was calculated from all rRT-PCR replicates of the tissue obtained from all animals infected with the same virus and euthanized at that timepoint. Additionally, a tissue-specific, timepoint-specific FMDV positive detection percentage (PDP) was defined and calculated from all animals infected with the same virus and euthanized at the same timepoint as: Number of Positive Test Results (VI or rRT-PCR) ÷ Number of Test Events (VI and rRT-PCR). Mean GCNs were statistically compared across experimental groups with student's *t*-test for means in GraphPad QuickCalcs software; PDPs were statistically compared across experimental groups using students *t*-test for proportions in Statistics Calculator 4.0 from StatPac. For both tests, the critical level for significance was defined as $p=0.05$. All comparisons not specifically indicated as "significant" in the text or figures, are purely descriptive (i.e. non-significant or statistical significance was not established).

Immunomicroscopy

Microscopic localization of FMDV antigens and host proteins was performed in cryosections as previously described (Arzt et al., 2009). Briefly, tissue sections were blocked for 2 h at 20 °C; primary antibodies were diluted in blocking buffer and applied to tissue sections for 18 h at 4 °C. For multichannel immunofluorescence (MIF), detection was performed with goat anti-rabbit and goat anti-mouse isotype-specific secondary antibodies labeled with AlexaFluor dyes (AF – 350, 488, 594, 647). Slides were examined with a wide-field, epifluorescence microscope, and images were captured with a cooled, monochromatic digital camera. Images of individual detection channels were adjusted for contrast and brightness and merged in commercially available software (Adobe Photoshop, CS2). Mouse monoclonal anti-FMDV-VP1 has been described previously (Baxt et al., 1989). Antibodies used to label cell markers in MIF experiments were mouse monoclonal anti-pancytokeratin plus (Biocare #CM162), anti-MHCII (AbD Serotec, MCA2225PE) and rabbit polyclonal anti-IFN-β (kindly provided by Dr. James Zhu).

For each MIF experiment, a duplicate, negative-control serial section treated with an isotype-matched irrelevant antibody or isotype control reagent of similar concentration was included. Additional negative control tissue sections were prepared from a steer that received a virus-free aerosol inoculum and was euthanized 72 hpa. MIF labeling was considered positive when there was an intense cell-associated signal within the experimental tissue with the absence of such staining in the negative controls.

Acknowledgments

This research was funded primarily by ARS-CRIS Project 1940-32000-057-00D. Additional funding came from an interagency agreement with the Science and Technology Directorate of the U.S. Department of Homeland Security under Award number HSHQDC-11-X-00189.

The authors wish to acknowledge Dr. James Zhu for providing anti-Bovine IFN-β. Madin-Darby bovine kidney-t2 (MDBK-t2) and Mx CAT ELISA technology were kindly provided by Dr. Bryan Charleston, Pirbright Institute. We thank Dr. Manuel Borca and Dr. Carolina Stenfeldt for critical review of the manuscript.

References

Alexandersen, S., Quan, M., Murphy, C., Knight, J., Zhang, Z., 2003. Studies of quantitative parameters of virus excretion and transmission in pigs and cattle experimentally infected with foot-and-mouth disease virus. J. Comp. Pathol. 129, 268–282.

Arzt, J., Baxt, B., Grubman, M.J., Jackson, T., Juleff, N., Rhyan, J., Rieder, E., Waters, R., Rodriguez, L.L., 2011a. The pathogenesis of foot-and-mouth disease II: viral pathways in swine, small ruminants, and wildlife; myotropism, chronic syndromes, and molecular virus-host interactions. Transbound Emerg. Dis. 58, 305–326.

Arzt, J., Gregg, D.A., Clavijo, A., Rodriguez, L.L., 2009. Optimization of immunohistochemical and fluorescent antibody techniques for localization of foot-and-mouth disease virus in animal tissues. J. Vet. Diagn. Invest. 21, 779–792.

Arzt, J., Juleff, N., Zhang, Z., Rodriguez, L.L., 2011b. The pathogenesis of foot-and-mouth disease I: viral pathways in cattle. Transbound Emerg. Dis. 58, 291–304.

Arzt, J., Pacheco, J.M., Rodriguez, L.L., 2010. The early pathogenesis of foot-and-mouth disease in cattle after aerosol inoculation: identification of the nasopharynx as the primary site of infection. Vet. Pathol. 47, 1048–1063.

Baxt, B., Vakharia, V., Moore, D.M., Franke, A.J., Morgan, D.O., 1989. Analysis of neutralizing antigenic sites on the surface of type A12 foot-and-mouth disease virus. J. Virol. 63, 2143–2151.

Belsham, G.J., 2013. Influence of the Leader protein coding region of foot-and-mouth disease virus on virus replication. J. Gen. Virol. 94, 1486–1495.

Borca, M.V., Pacheco, J.M., Holinka, L.G., Carrillo, C., Hartwig, E., Garriga, D., Kramer, E., Rodriguez, L., Piccone, M.E., 2012. Role of arginine-56 within the structural protein VP3 of foot-and-mouth disease virus (FMDV) O1 Campos in virus virulence. Virology 422, 37–45.

Brown, C.C., Piccone, M.E., Mason, P.W., McKenna, T.S., Grubman, M.J., 1996. Pathogenesis of wild-type and leaderless foot-and-mouth disease virus in cattle. J. Virol. 70, 5638–5641.

Callahan, J.D., Brown, F., Osorio, F.A., Sur, J.H., Kramer, E., Long, G.W., Lubroth, J., Ellis, S.J., Shoulars, K.S., Gaffney, K.L., Rock, D.L., Nelson, W.M., 2002. Use of a portable real-time reverse transcriptase-polymerase chain reaction assay for rapid detection of foot-and-mouth disease virus. J. Am. Vet. Med. Assoc. 220, 1636–1642.

Chinsangaram, J., Mason, P.W., Grubman, M.J., 1998. Protection of swine by live and inactivated vaccines prepared from a leader proteinase-deficient serotype A12 foot-and-mouth disease virus. Vaccine 16, 1516–1522.

Chinsangaram, J., Moraes, M.P., Koster, M., Grubman, M.J., 2003. Novel viral disease control strategy: adenovirus expressing alpha interferon rapidly protects swine from foot-and-mouth disease. J. Virol. 77, 1621–1625.

Chinsangaram, J., Piccone, M.E., Grubman, M.J., 1999. Ability of foot-and-mouth disease virus to form plaques in cell culture is associated with suppression of alpha/beta interferon. J. Virol. 73, 9891–9898.

de los Santos, T., Diaz-San Segundo, F., Grubman, M.J., 2007. Degradation of nuclear factor kappa B during foot-and-mouth disease virus infection. J. Virol. 81, 12803–12815.

Diaz-San Segundo, F., Moraes, M.P., de Los Santos, T., Dias, C.C., Grubman, M.J., 2010. Interferon-induced protection against foot-and-mouth disease virus infection

correlates with enhanced tissue-specific innate immune cell infiltration and interferon-stimulated gene expression. J. Virol. 84, 2063–2077.
Diaz-San Segundo, F., Weiss, M., Perez-Martin, E., Koster, M.J., Zhu, J., Grubman, M.J., de los Santos, T., 2011. Antiviral activity of bovine type III interferon against foot-and-mouth disease virus. Virology 413, 283–292.
Fray, M.D., Mann, G.E., Charleston, B., 2001. Validation of an Mx/CAT reporter gene assay for the quantification of bovine type-I interferon. J. Immunol. Methods 249, 235–244.
Gladue, D.P., O'Donnell, V., Baker-Branstetter, R., Holinka, L.G., Pacheco, J.M., Fernandez-Sainz, I., Lu, Z., Brocchi, E., Baxt, B., Piccone, M.E., Rodriguez, L., Borca, M.V., 2012. Foot-and-mouth disease virus nonstructural protein 2C interacts with Beclin1, modulating virus replication. J. Virol. 86, 12080–12090.
Grubman, M.J., Baxt, B., 2004. Foot-and-mouth disease. Clin. Microbiol. Rev. 17, 465–493.
Henderson, W., 1949. The Quantitative Study of Foot-and-Mouth Disease Virus. Agricultural Research Council, Report Series 8.
Howey, R., Bankowski, B., Juleff, N., Savill, N.J., Gibson, D., Fazakerley, J., Charleston, B., Woolhouse, M.E., 2012. Modelling the within-host dynamics of the foot-and-mouth disease virus in cattle. Epidemics 4, 93–103.
Lawrence, P., Schafer, E.A., Rieder, E., 2012. The nuclear protein Sam68 is cleaved by the FMDV 3C protease redistributing Sam68 to the cytoplasm during FMDV infection of host cells. Virology 425, 40–52.
Moraes, M.P., de Los Santos, T., Koster, M., Turecek, T., Wang, H., Andreyev, V.G., Grubman, M.J., 2007. Enhanced antiviral activity against foot-and-mouth disease virus by a combination of type I and II porcine interferons. J. Virol. 81, 7124–7135.
Muller-Doblies, D., Ackermann, M., Metzler, A., 2002. In vitro and in vivo detection of Mx gene products in bovine cells following stimulation with alpha/beta interferon and viruses. Clin. Diagn. Lab. Immunol. 9, 1192–1199.
Pacheco, J.M., Arzt, J., Rodriguez, L.L., 2010a. Early events in the pathogenesis of foot-and-mouth disease in cattle after controlled aerosol exposure. Vet. J. 183, 46–53.
Pacheco, J.M., Gladue, D.P., Holinka, L.G., Arzt, J., Bishop, E., Smoliga, G., Pauszek, S.J., Bracht, A.J., O'Donnell, V., Fernandez-Sainz, I., Fletcher, P., Piccone, M.E., Rodriguez, L.L., Borca, M.V., 2013. A partial deletion in non-structural protein 3A can attenuate foot-and-mouth disease virus in cattle. Virology 446, 260–267.
Pacheco, J.M., Piccone, M.E., Rieder, E., Pauszek, S.J., Borca, M.V., Rodriguez, L.L., 2010b. Domain disruptions of individual 3B proteins of foot-and-mouth disease virus do not alter growth in cell culture or virulence in cattle. Virology 405, 149–156.
Perez-Martin, E., Weiss, M., Diaz-San Segundo, F., Pacheco, J.M., Arzt, J., Grubman, M.J., de los Santos, T., 2012. Bovine type III interferon significantly delays and reduces the severity of foot-and-mouth disease in cattle. J. Virol. 86, 4477–4487.
Pfaffl, M.W., 2001. A new mathematical model for relative quantification in real-time RT-PCR. Nucleic Acids Res. 29, e45.
Piccone, M.E., Diaz-San Segundo, F., Kramer, E., Rodriguez, L.L., de los Santos, T., 2010a. Introduction of tag epitopes in the inter-AUG region of foot and mouth disease virus: effect on the L protein. Virus Res. 155, 91–97.
Piccone, M.E., Pacheco, J.M., Pauszek, S.J., Kramer, E., Rieder, E., Borca, M.V., Rodriguez, L.L., 2010b. The region between the two polyprotein initiation codons of foot-and-mouth disease virus is critical for virulence in cattle. Virology 396, 152–159.
Reid, E., Juleff, N., Gubbins, S., Prentice, H., Seago, J., Charleston, B., 2011. Bovine plasmacytoid dendritic cells are the major source of type I interferon in response to foot-and-mouth disease virus in vitro and in vivo. J. Virol. 85, 4297–4308.
Rieder, E., Henry, T., Duque, H., Baxt, B., 2005. Analysis of a foot-and-mouth disease virus type A24 isolate containing an SGD receptor recognition site in vitro and its pathogenesis in cattle. J. Virol. 79, 12989–12998.
Sadler, A.J., Williams, B.R., 2008. Interferon-inducible antiviral effectors. Nat. Rev. 8, 559–568.
Sommereyns, C., Paul, S., Staeheli, P., Michiels, T., 2008. IFN-lambda (IFN-lambda) is expressed in a tissue-dependent fashion and primarily acts on epithelial cells in vivo. PLoS Pathog. 4, e1000017.
Stenfeldt, C., Heegaard, P.M., Stockmarr, A., Belsham, G.J., 2012. Modulation of cytokine mRNA expression in pharyngeal epithelial samples obtained from cattle infected with foot-and-mouth disease virus. J. Comp. Pathol. 146, 243–252.
Stenfeldt, C., Heegaard, P.M., Stockmarr, A., Tjornehoj, K., Belsham, G.J., 2011. Analysis of the acute phase responses of Serum Amyloid A, Haptoglobin and Type 1 Interferon in cattle experimentally infected with foot-and-mouth disease virus serotype O. Vet. Res. 42, 66.
Taubert, A., Zahner, H., Hermosilla, C., 2006. Dynamics of transcription of immunomodulatory genes in endothelial cells infected with different coccidian parasites. Vet. Parasitol. 142, 214–222.
Uddowla, S., Hollister, J., Pacheco, J.M., Rodriguez, L.L., Rieder, E., 2012. A safe foot-and-mouth disease vaccine platform with two negative markers for differentiating infected from vaccinated animals. J. Virol. 86, 11675–11685.
Zhang, Z., Ahmed, R., Paton, D., Bashiruddin, J.B., 2009. Cytokine mRNA responses in bovine epithelia during foot-and-mouth disease virus infection. Vet. J. 179, 85–91.
Zhang, Z., Bashiruddin, J.B., Doel, C., Horsington, J., Durand, S., Alexandersen, S., 2006. Cytokine and toll-like receptor mRNAs in the nasal-associated lymphoid tissues of cattle during foot-and-mouth disease virus infection. J. Comp. Pathol. 134, 56–62.
Zhu, J.J., Arzt, J., Puckette, M.C., Smoliga, G.R., Pacheco, J.M., Rodriguez, L.L., 2013. Mechanisms of foot-and-mouth disease virus tropism inferred from differential tissue gene expression. PLoS One 8, e64119.